Article:
Gauer, JS orcid.org/0000-0002-0835-639X, Tumova, S orcid.org/0000-0003-2044-4998, Lippiat, JD orcid.org/0000-0003-3748-7345 et al. (2 more authors) (2018) Differential patterns of inhibition of the sugar transporters GLUT2, GLUT5 and GLUT7 by flavonoids. Biochemical Pharmacology, 152. pp. 11-20. ISSN 0006-2952

https://doi.org/10.1016/j.bcp.2018.03.011

Differential patterns of inhibition of the sugar transporters GLUT2, GLUT5 and GLUT7 by flavonoids

*Corresponding author: g.williamson@leeds.ac.uk

Phone +44 113 3438380; Email: g.williamson@leeds.ac.uk

Contribution of authors:

JSG: Performed all experimental work, planned and designed research, analysed data.

JDL: Provided expertise and advice on *X. laevis* oocyte microinjection.

ST: Provided cell culture expertise and optimized conditions for quantitative Western blotting.

AK: Planning of research, radiochemistry expertise, and advice on experimental work.

GW: Supervised, planned and designed research.

Writing of paper: First draft written by JSG. All authors have contributed, read and agreed to the contents of the manuscript.

Abbreviations:

GLUT2: solute carrier family 2, member 2 (SLC2A2), human

GLUT5: solute carrier family 2, member 5 (SLC2A5), human

GLUT7: solute carrier family 2, member 7 (SLC2A7), human

SGLT1: Sodium-dependent sodium-glucose cotransporter 1

EGCG: (–)-epigallocatechin-gallate

IVT: in vitro transcription

ddPCR: digital droplet polymerase chain reaction

FBS: fetal bovine serum

DAPI: 4',6-diamidino-2-phenylindole

WGA: Wheat Germ Agglutinin

ABSTRACT

Only limited data are available on the inhibition of the sugar transporter GLUT5 by flavonoids or other classes of bioactives. Intestinal GLUT7 is poorly characterised and no information exists concerning its inhibition. We aimed to study the expression of GLUT7 in Caco-2/TC7 intestinal cells, and evaluate inhibition of glucose transport by GLUT2 and GLUT7, and of fructose transport by GLUT2, GLUT5 and GLUT7, by flavonoids. Differentiated Caco-2/TC7 cell monolayers were used to investigate GLUT7 expression, as well as biotinylation and immunofluorescence to assess GLUT7 location. For mechanistic sugar transport studies, X. laevis oocytes were injected with individual mRNA, and GLUT protein expression on oocyte membranes was confirmed. Oocytes were incubated with D-[^{14}C(U)]-glucose or D-[^{14}C(U)]-fructose in the presence of flavonoids, and uptake was estimated by liquid scintilation counting. In differentiated Caco-2/TC7 cell monolayers, GLUT7 was mostly expressed apically. When applied apically, or to both compartments, sorbitol, galactose, L-glucose or sucrose did not affect GLUT7 mRNA expression. Fructose applied to both sides increased GLUT7 mRNA (13%, $p \leq 0.001$) and total GLUT7 protein (2.7-fold, $p \leq 0.05$), while the ratio between apical, basolateral and total GLUT7 protein was unchanged. In the X. laevis oocyte model, GLUT2-mediated glucose and fructose transport were inhibited by quercetin, (-)-epigallocatechin gallate (EGCG) and apigenin, GLUT5-mediated fructose transport was inhibited by apigenin and EGCG, but not by quercetin, and GLUT7-mediated uptake of both glucose and fructose was inhibited by apigenin, but not by quercetin nor EGCG. Expression of GLUT7 was increased by fructose, but only when applied to Caco-2/TC7 cells both apically and basolaterally. Since GLUT2, GLUT5 and GLUT7 show different patterns of inhibition by the tested flavonoids, we suggest that they have the potential to be used as investigational tools to distinguish sugar transporter activity in different biological settings.

Key words: polyphenols; Xenopus laevis oocytes; sugar transporters; flavonoids; Caco-2 cells

1. INTRODUCTION

GLUT proteins are members of the SLC2 family and transport monosaccharides and polyols across eukaryotic cell membranes by a facilitative mechanism but with different affinity and specificity. Intestinal glucose absorption across the apical membrane involves both sodium-glucose cotransporter 1 (SGLT1) and GLUT2 [1, 2], while transport of glucose to the blood is catalysed by GLUT2 on the basolateral membrane [3]. In the presence of high glucose concentrations, transport is mediated primarily by GLUT2 rather than SGLT1, through trafficking of additional GLUT2 to the apical surface [4, 5]. This mechanism is supported by evidence showing, for example, that GLUT2 is localised to the apical membrane in rat intestinal models with elevated sugar concentrations [6]. Fructose uptake in the gut is primarily mediated by GLUT5 which recognizes all forms of the sugar [7-9]. Secondary fructose transport is facilitated by GLUT2, which is able to recognize fructose in its furanose form [10], and is responsible for transporting absorbed fructose across the basolateral membrane of enterocytes and into the blood [11]. GLUT7 is expressed in the intestine and very few other tissues, and is the closest relative to GLUT5, sharing 53% sequence homology and 68% amino acid identity [12, 13]. GLUT7 has a notably high affinity for both glucose and fructose (< 0.5 mM), and due to high levels of expression in the ileum, may be responsible for sugar uptake at the end of a meal, when sugar concentrations gradually decrease [14-16]. Although there is still controversy about the ability of GLUT7 to transport sugars [17, 18], two studies on expression of human GLUT7 in *X. laevis* oocytes reported that this protein was able to transport fructose and glucose, but not galactose [12, 15]. It has been hypothesised that a conserved motif, present in the sequences of GLUT2, GLUT5 and GLUT7, is responsible for their ability to transport fructose [18-20].

Many flavonoids have been shown to inhibit GLUT2, including tiliroside, myricetin, phloretin, EGCG and apigenin [21] [22] [23] [24]. Quercetin is also a potent inhibitor of both glucose and fructose uptake by GLUT2, through binding to a non-sugar binding site [23] [25]. Unlike GLUT2, inhibition of GLUT5 sugar uptake has only been shown for a limited number of flavonoids: (–)-epicatechin-gallate (ECG) and (–)-epigallocatechin-gallate (EGCG) [26]. The sugar analogue L-sorbose-Bn-OZO also inhibits GLUT5, and contains a bulky benzyl group thought to bind to a position out of the binding site. The oxygen molecule in the OZO moiety increases hydrogen interactions with the protein, allowing for tighter binding [8]. No inhibitors of GLUT7 of any type have yet been reported, and, in fact, even the ability of GLUT7 to transport sugars has been questioned [17, 18].

2. MATERIALS AND METHODS

2.1 Chemicals

D-[^{14}C(U)]-glucose was from Perkin Elmer (Boston, USA), D-[^{14}C(U)]-fructose was from Hartmann Analytic (Braunschweig, Germany), and D-fructose, D-glucose and Glutamax™ were from Thermo Fisher Scientific (Paisley, UK). Dulbeccos's modified Eagle's Medium, fetal bovine serum (FBS), non-essential amino acids, penicillin, protease inhibitor cocktail and streptomycin were from Sigma-Aldrich, UK. L-sorbose-Bn-OZO was kindly provided by Professor Arnaud Tatibouet, Université d'Orléans, France.

2.2 Cell culture

Caco-2/TC7 cells at passage number 30 and kindly donated by Dr M. Rousset (U178 INSERM, Villejuif, France), were routinely cultured in 25 mM glucose Dulbeccos's modified Eagle's Medium supplemented with 20% (v/v) fetal bovine serum (FBS), 2% (v/v) Glutamax™, 2% (v/v) non-essential amino acids, 100 U/mL penicillin and 0.1 mg/mL streptomycin at 37 °C

with 10% CO_2 in a humidified atmosphere. Cells were used between passage numbers 30 and 40.

2.3 Gene expression analysis using digital droplet PCR

Caco-2/TC7 cells were seeded on 6-well Transwell plates (0.4 μm pore size, polycarbonate, Corning, UK) at a density of 6×10^4 cm^{-2} and maintained for 21 d in the conditions indicated above. After 7 d post-seeding and up to 21 d cells were grown in asymmetric conditions, with FBS included only in the medium added to the basolateral side of each well. Throughout the differentiation period (7-21 d), cells were grown in the standard glucose medium or in medium supplemented with 25 mM of one of the following sugars; fructose, sorbitol, galactose, L-glucose and sucrose on apical side only, or on both apical and basolateral sides. At day 21 cells were lifted and mRNA was extracted using the Aurum Total RNA Mini Kit (Bio-Rad, UK), following manufacturer's instructions. Reverse transcription of RNA to cDNA was performed with a high capacity RNA to cDNA kit (Applied Biosystems, Life Technologies, USA). Droplet digital PCR (ddPCR) was used to quantitatively determine gene expression using TaqMan duplexed FAM/VIC assays in a QX100 system (Bio-Rad), as previously described [27]. Triplicate reactions of 20 µL stock sample solution were prepared by adding 8 µL total transcribed nucleic acids (5 ng) diluted with MilliQ water, 1 µL GLUT7 (SLC2A7) FAM™-labelled TaqMan primer (Hs01013553_m1, Thermo Fisher Scientific, UK) and 10 µL of ddPCR Supermix for Probes (Bio-Rad). In addition, 1 µL VIC™-labelled probe for TBP (TATA box binding protein, Hs00427620_m1) (Thermo Fisher Scientific, UK) was added to final sample solution to act as a reference. All data were analysed with the QuantaSoft software (Kosice, Slovakia). Concentrations of target and reference cDNA (Tata Binding Box Protein 1, TBP) measured as copies/µL are presented as a ratio.

2.4 Protein expression analysis by cell surface biotinylation

Cell surface biotinylation was performed using the Pierce Cell Surface Protein Isolation Kit (89881, Thermo Fisher Scientific, UK) according to the manufacturer's instructions. Briefly, cells were washed twice with ice cold phosphate buffered saline with calcium chloride and magnesium chloride (PBS+) (D1283, Sigma-Aldrich, UK) before incubation with 0.25 mg/ml Sulfo-NHS-SS-Biotin for 30 min, on ice, on a low speed shaker. Quenching solution was added to each well, and cells were washed twice with Tris buffered saline (TBS) buffer (1706435, Bio-Rad, UK). Cells were scraped and lysed on ice for 30 min in 60 mM octylglucoside/150 mM NaCl/20 mM Tris solution (pH 7.4), containing protease inhibitors. Following centrifugation at 14,000 g for 5 min supernatant was transferred into a new tube and protein concentration for each cell lysate was determined with a ND100 Nanodrop spectrophotometer (Thermo Fisher Scientific, UK). NeutrAvidin Agarose beads in Pierce Spin Columns (Thermo Fisher Scientific, UK) were washed twice with TBS and lysis buffer. Lysates were added to the filter columns at comparable protein concentrations, and incubated at room temperature on a rotator at low speed for 1 h. Filter columns were washed twice with TBS and then treated with Rapid PNGase F (P0710S, New England Biolabs, USA) for 15 min at 37 °C to remove N-glycosylation. Biotinylated membrane fractions were eluted with SDS-PAGE buffer containing 0.5 M dithiothreitol following a 20 min incubation at 37 °C..

2.5 Immunofluorescence staining

Caco-2/TC7 cells were seeded at a density of 6 x 10^4 cm^2 on Millicell cell culture inserts (12-well, PET 0.4 mm pore size, Millipore) and maintained as described above for 21 d. Cells were fixed with 4% para-formaldehyde in phosphate buffered saline (PBS) and incubated with 5 µg/mL Fluorescein labelled Wheat Germ Agglutinin (WGA) (Fl-1021, Vector Laboratories, Peterborough, UK) for 10 min at 37 °C. Cells were then washed three times with PBS+ and

permeabilised with 0.1% Triton-X100 for 20 min at room temperature before incubation with GLUT7 primary antibody (NBP1-81821, Novus Biologicals, USA) at a 1:50 dilution for 1 h at room temperature. After three washes with PBS, cells were incubated with Cy3-conjugated AffiniPure donkey anti-rabbit IgG (711-165-152, Jackson ImmunoResearch, USA) secondary antibody at a dilution of 1:300. Cells were washed three times with PBS, stained with 2 µg/mL 4',6-diamidino-2-phenylindole (DAPI) for 5 min, rinsed with water, and mounted onto microscopy slides using ProLong Gold antifade reagent mounting medium (Thermo Fisher Scientific, UK). Images were obtained with a Zeiss LSM 700 Inverted Confocal Microscope using the 63x lens objective. Cells imaged without WGA were permeabilized once fixed and processed for imaging in the same way as described above, with the exception that Alexa Fluor 488-conjugated AffiniPure donkey anti-rabbit IgG (711-545-152, Jackson ImmunoResearch, USA), at a dilution of 1:300, was used in the secondary antibody incubation step.

2.6 Protein expression analysis in Caco-2/TC7 cells by automated western blotting

Expression of membrane-localised GLUT7 after biotinylation was determined using automated capillary Western blotting (WES, ProteinSimple, Bio-Techne, UK). Cell lysates were treated with Rapid PNGase F for 15 min prior to the denaturation step (37 °C, 15 min). GLUT7 antibody (NBP1-81821, Novus Biologicals, USA) was diluted 1:10 and Na^+/K^+ ATPase (#3010, New England Biolabs Ltd, UK) diluted 1:100 was used as a loading control. Optimal loading concentration for the cell lysate samples was 0.4 mg of total protein/mL. The membrane fraction of biotinylated samples was analysed without dilution.

2.7 Isolation of mRNA encoding GLUT2, GLUT5 and GLUT7 genes

Human GLUT2 and GLUT5 mRNA were obtained following methods previously described [22]. Human GLUT7 mRNA was prepared from GLUT7pGEM-HE plasmid, kindly supplied by Debbie O'Neill of Prof. Chris Cheeseman's group (Department of Physiology, Alberta University, Canada). The plasmid was linearized with NheI (R6501, Promega, WI, USA) before being added to the T7 polymerase mMESSAGE mMACHINE® (AM1344, Ambion, Applied Biosystems, UK) in vitro transcription kit to produce capped RNA products.

2.8 Preparation of Xenopus laevis oocytes for microinjections

X. laevis oocytes were isolated and microinjected as described previously [22]. Following microinjections, oocytes were kept at 18 ^{o}C in ND96-ACT medium for 24 h (GLUT5-injected oocytes), 48 h (GLUT2-injected oocytes) or 120 h (GLUT7-injected oocytes) before experiments were carried out.

2.9 Specificity of mRNA products

Plasmids were specifically designed to ensure that the protein coding sequence of both GLUT2 and GLUT5 were placed in between the SP6 promoter and a unique restriction enzyme site. The GLUT7 gene coding region was placed between the T7 promoter and a specific restriction enzyme site in the provided GLUT7pGEM-HE plasmid. To determine mRNA quality and specificity, samples obtained from the in vitro transcription (IVT) steps were run on a formaldehyde RNA denaturing gel to confirm the size of the mRNA products.

2.10 Protein expression analysis in X. laevis oocytes by automated western blotting

Membranes from oocytes microinjected with protein mRNA or water were extracted following post-microinjection incubation (24 h for GLUT5, 48 h for GLUT2, or 120 h for GLUT7). For GLUT2 and GLUT7, times were chosen based on published literature [12, 23]. For GLUT5, a preliminary analysis of expression in oocytes was carried out between 1-5 days post micro-injection, which indicated highest expression at day 1. Expression of human GLUT2, GLUT5 and GLUT7 in Xenopus laevis oocyte membranes was determined by automated capillary western blotting according to manufacturer's instructions, as previously described [28], with the exception of the sample denaturing conditions (37 °C for 15 min). Membrane extracts of GLUT2- and GLUT7-injected oocytes were treated with Rapid PNGase F (New England Biolabs, USA) for 15 min prior to the denaturation step. GLUT2 (ab95256, Abcam, UK) and GLUT5 antibodies (sc271055, Santa Cruz Biotechnology, USA) were diluted 1:50. Optimal loading concentration for GLUT2 and GLUT5 oocyte membrane samples was 0.4 mg/mL and 0.2 mg/mL respectively. GLUT7 antibody was diluted 1:10. Membrane extracts of GLUT7-expressing oocytes were used undiluted.

2.11 Glucose and fructose uptake by oocytes expressing GLUT2, GLUT5 or GLUT7

Following microinjection with protein mRNA or water, Xenopus laevis oocytes were incubated in 100 µM 0.5 µCi/mL D-[^{14}C(U)]-glucose (GLUT2, GLUT7) or D-[^{14}C(U)]-fructose (GLUT2, GLUT5 and GLUT7). Incubations were carried out at 25 °C for 5, 15 or 30 min. To terminate the incubation, oocytes were washed with ice cold 100 µM sugar solution and homogenised in 0.3 M sucrose containing 10 mM sodium phosphate and a protease inhibitor mixture. Where possible, time points were chosen to best reflect the linear portion of the uptake against time curve. Either 3 oocytes (GLUT2 and GLUT5) or 10 oocytes (GLUT7) were homogenised together. In order to separate the yolk and pellet cell debris, the homogenized

samples were centrifuged at 3,000 g for 15 min at 4 °C. The supernatant was centrifuged at 48,000 g for 1 h at 4 °C to pellet the membranes, which were re-suspended in the same solution used for the homogenisation step and stored at –20 °C until protein expression analysis. The supernatant of the second centrifugation step was added to a vial containing 5 ml of scintillation fluid and radioactivity was measured using a Packard Tri-Carb 1900 TR Liquid Scintillation Counter. Samples not used for protein analysis were homogenised and directly assessed by scintillation counting as neither the yolk or cell debris interfered with measurements, as determined in preliminary tests.

2.12 Statistics

Oocyte sugar uptake experiments involved six replicates of 3 oocytes, or three replicates of 10 oocytes, per individual condition. Importantly, water-injected control oocytes were used in every experiment and for each and every individual condition. Each data point represents the mean of all replicates ± SEM, normalized to the mean of respective controls, except when controls are included in the figures. Two tailed homoscedastic Student's t-test was used to test significance, as previously reported [19]. IC_{50} values were the average concentration of the replicate determinations of the added compound at which the uptake of sugar by each replicate was decreased by 50%. For protein and gene expression in Caco-2/TC7 cells, each data point represents the mean of three biological replicates, and three technical replicates in gene expression assays, ± SEM. Cells cultured in standard glucose medium were used as controls for all experiments. Data from biological replicates were combined by normalizing each individual experiment to the control and ANOVA was performed to determine statistical differences. Two tailed homoscedastic Student's t-test was used to test significance.

3. RESULTS

3.1 Localisation of GLUT7 on Caco-2/TC7 cellular membranes by immunostaining

GLUT7 mRNA was expressed at higher levels in the Caco-2/TC7 clone compared to parental Caco-2 cells (259 ± 77 cf 87 ± 8 copies/ng of cDNA), and so the former was used for subsequent experiments. Immunostaining with anti-GLUT7 primary antibody showed GLUT7 protein localization (green or red fluorescence) mainly on the apical membrane (figure 1), with less on the lateral membrane, and very little on the basal membrane. The possibility of GLUT7 being expressed on the apical brush border membrane, due to the high sequence similarity with GLUT5, has been previously proposed [15] [12]. In addition, immunohistochemical analyses localized rat GLUT7 to the apical membrane of small intestinal epithelial cells [15].

3.2 Modulation of expression of GLUT7 in Caco-2/TC7 cells

Expression of GLUT7 in Caco-2/TC7 cells grown in media supplemented with fructose, sorbitol, galactose, L-glucose or sucrose on the apical side during the cell differentiation period (7-21 d) remained unchanged when compared to the glucose control (figure 2 A). In comparison, in cells grown in media supplemented with fructose (but not the other sugars) on both apical and basolateral sides showed a small but significant increase (13%, $p \leq 0.001$) in GLUT7 mRNA expression was noted when compared to glucose control (figure 2 B). In Caco-2/TC7 cells GLUT7 was readily detected as a single band of 49 kDa, following treatment with PNGase, and could be analysed in the same capillary with Na^+K^+ATPase, with both proteins showing a linear response with increasing protein concentration (figure 2 C and D). GLUT7 protein expression in cell lysates, normalized to Na^+K^+ATPase [29], increased 2.7-fold ($p \leq 0.05$) (figure 2 E), however, this did not change the ratio between apical and total, nor basolateral and total, GLUT7 protein, as assessed by biotinylation (figure 2 F). The expression

of GLUT7 on the apical surface of differentiated Caco-2/TC7 cell monolayers makes the model amenable to flavonoid inhibition. The flavonoids EGCG, apigenin and quercetin can attenuate transport of glucose and fructose across differentiated Caco-2 and Caco-2/TC7 cell monolayers [22] [24], but these cells, as for the intestine in vivo, express a variety of GLUT and other sugar transporters, which makes the determination of the role of individual transporters difficult. We therefore used the Xenopus laevis expression system to elucidate effects of flavonoid inhibitors on individual functional GLUTs.

3.3 GLUT protein expression in Xenopus laevis oocyte membranes and transport of sugars

We expressed human GLUT2, GLUT5 and GLUT7 in X. laevis oocytes. Sizes of injected mRNA encoding for each GLUT were confirmed by analyses on an RNA formaldehyde gel. After injection and incubation to allow for protein synthesis, GLUT2 or GLUT5 proteins were clearly detected in membrane extracts of oocytes injected with mRNA, but not of water-injected controls (figure 3 A, B, D and E). The predicted M_r of human GLUT7 is 55.7 kDa, with an N-glycosylation site at residue 57. A band of M_r = 59 kDa was observed after expression of GLUT7 in oocytes, together with a dominant non-specific band derived from the oocyte membrane (figure 3). After removal of N-glycans by PNGase, the 59 kDa band shifted to a lower molecular weight, consistent with removal of N-glycosylation (figure 3 C and F). Furthermore, oocytes expressing GLUT2 and GLUT7 were able to take up D-[^{14}C(U)]-glucose, and those expressing GLUT5 and GLUT7 could take up D-[^{14}C(U)]-fructose. L-sorbose-Bn-OZO, reported to inhibit GLUT5 [8], inhibited GLUT5-mediated fructose uptake by more than 50%, $p \leq 0.01$ (figure 4 A). GLUT2-mediated glucose uptake was inhibited by both cytochalasin B (70% inhibition at 100 µM, $p \leq 0.0001$) and phloretin (81 % inhibition at 100 µM, $p \leq 0.0001$) as expected (figure 4 B). To date, there have been no accounts of GLUT7

inhibitors, with compounds such as phloretin and cytochalasin B having no impact on glucose uptake by this transporter (figure 4 C), as previously demonstrated [12]. Based on the protein data, we predict that GLUT7 protein was expressed at a lower level compared to GLUT2 and GLUT5.

3.4 Inhibition of glucose and fructose transport in Xenopus laevis oocytes expressing GLUT2

EGCG and apigenin dose-dependently inhibited GLUT2, decreasing uptake of both D-[^{14}C(U)]-glucose and of D-[^{14}C(U)]-fructose (figure 5 A, B; Table 1). Quercetin was also a potent inhibitor, as previously reported [23] (figure 5 C).

3.5 Inhibition of fructose transport in Xenopus laevis oocytes expressing GLUT5

EGCG and apigenin inhibited uptake of 0.1 mM D-[^{14}C(U)]-fructose into oocytes expressing GLUT5 (figure 6 A and B; Table 1). Quercetin did not have any significant effect on fructose uptake by GLUT5 at any of the concentrations tested (figure 6 C), as previously reported [23].

3.6 Inhibition of glucose and fructose transport in Xenopus laevis oocytes expressing GLUT7

Uptake of D-[^{14}C(U)]-glucose and D-[^{14}C(U)]-fructose by GLUT7-expressing oocytes was unchanged in the presence of EGCG even at high concentrations (figure 7 A). Apigenin significantly, and concentration-dependently, inhibited GLUT7-mediated D-[^{14}C(U)]-fructose uptake (Table 1). GLUT7-mediated D-[^{14}C(U)]-glucose uptake was also significantly inhibited by apigenin, (figure 7 B; Table 1). There was no significant change in D-[^{14}C(U)]-fructose or D-[^{14}C(U)]-glucose uptake by GLUT7-expressing oocytes in the presence of quercetin up to 100 µM (figure 7 C).

298

299

4. DISCUSSION

Sugar transporters have multiple functions in cells, and only some transport glucose across membranes [30-32]. The role of GLUT7, predominantly expressed in the intestine, is still controversial and its physiological function remains unclear [30]. As the closest related protein to GLUT5, GLUT7 is also proposed to be a fructose transporter [15, 33]. Nevertheless, contradictory data on the capability of GLUT7 to transport fructose and glucose have been reported [12, 17, 18], and no inhibitors are known. Our data clearly demonstrates that GLUT7 expressed in oocytes is able to transport both glucose and fructose, in agreement with other data on microinjected GLUT7-expressing oocytes [12]. However, this is in contrast to the work of one group where sugar uptake by oocytes expressing GLUT7 could not be detected [17, 18]. If we closely examine the methodology, several major differences become apparent to the work described here: we injected almost 4-fold higher amount of RNA, and we also used water-injected oocytes as blanks, rather than non-injected oocytes. Water injection provides a control for the microinjection procedure, which leads to a development of the pigmented ring scar caused by the micropipette prick and can affect the membrane permeability [34]. Low amounts of sugar are able to influx through this scar on the oocyte surface, as determined by radioactivity measurements of water-injected oocytes versus non-injected oocytes, the latter producing radioactivity counts equivalent to background levels. To account for the amount of uptake caused by the scar produced during microinjection, as well as any change in membrane permeability from the contents of each compound, all uptake data presented here was normalized to control water-injected oocytes that were exposed to the same conditions as mRNA-injected oocytes. Moreover, we tested the protein expression and sugar uptake in GLUT7 microinjected oocytes over several days post-injection and found that a longer incubation time of 5 d was essential to result in stable expression. It is notable that, in our hands, the GLUT7-catalysed sugar transport showed more variation between experiments

compared to GLUT2 and GLUT5, but the reason for this is not clear. Furthermore, in support of GLUT7 activity, we observed no inhibition by phloretin nor cytochalasin B, in agreement with previous observations [12]. By confirming that fructose is, in fact, transported by GLUT7, our results also fit with the hypothesis that a conserved isoleucine-containing motif present in GLUT2, GLUT5 and GLUT7 may be essential for the transport of fructose [19]. Consistent with potential involvement in sugar transport across the membrane, immunostaining showed that GLUT7 transporter protein is primarily localized to the apical membrane of differentiated Caco-2/TC7 monolayers, with less GLUT7 present on the basal side.

It would be anticipated that expression of sugar transporters could be modulated by sugars, and as an example, expression of both GLUT2 and GLUT5 was increased in the presence of glucose and fructose, respectively [35, 36]. Here we found that only apical and basolateral fructose, and not the other sugars tested, induced both GLUT7 mRNA and total protein in differentiated Caco-2/TC7 cells. The increased protein concentration in the cell did not change the ratio between surface-expressed and total protein, implying that the increase was due to more protein synthesis or less degradation, and not enhanced trafficking per se.

Having confirmed that GLUT7 can transport fructose and glucose, we then tested if it could be inhibited by flavonoids. We show for the first time that apigenin, but not EGCG nor quercetin, was an effective inhibitor of GLUT7 glucose and fructose transport. In comparison, GLUT2 was inhibited by all three flavonoids tested, and the extent of inhibition by quercetin was comparable to that previously reported [23]. For GLUT5, EGCG and apigenin were effective inhibitors, but quercetin was not. The lack of inhibition by quercetin and inhibition by EGCG are in agreement with other studies on GLUT5 [23, 26]. Since the oocyte model indicates interaction with the expressed protein, then we would expect that all of the observed inhibition

reactions are due to direct binding of the flavonoid to the sugar transporter. Some flavonoids are able to inhibit other GLUTs, and, for example, EGCG inhibits GLUT1 and SGLT1 [24, 26], and quercetin inhibits the "class 1" transporters GLUT1, 2 and 4 [23, 37, 38]. Based on the previous observations and the data presented here, it is suggested that flavonoids have the potential to modulate glucose transport by inhibition of GLUT transporters, and that the specificity of inhibition could be exploited in mechanistic studies to examine the role of sugar transporters in cells.

Acknowledgments

We acknowledge funding from the European Research Council as an advanced grant (POLYTRUE? 322467). We thank Dr Samantha Gardner and Dr Lyn McKeown for their contribution to plasmid design, Professor Arnaud Tatibouet from the Université d'Orléans, France, for kindly proving the GLUT5 inhibitor, and Professor Chris Cheeseman from Alberta University, Canada, for kindly supplying the GLUT7pGEM-HE plasmid.

Table 1. Summary of data on inhibition of GLUTs by flavonoids

	GLUT2		GLUT5	GLUT7	
	glucose	fructose	fructose	glucose	fructose
Apigenin (μM)	27 ± 4	28 ± 10	40 ± 4	~38 *	16 ± 12
Quercetin (μM)	7 ± 1	8 ± 2	NI	NI	NI
EGCG (μM)	72 ± 13	93 ± 16	72 ± 13	NI	NI

* Inhibition did not follow a clear dose-dependency (see Fig. 7B) and so the IC_{50} value was estimated from zero and highest concentration of compound tested. NI = no inhibition observed. Data are ± standard deviation.

Figure 1. Immunofluorescence detection of GLUT7 in differentiated Caco-2/TC7 monolayers. Cells were incubated with nuclear stain DAPI (blue), rabbit anti-GLUT7 primary antibody and either Cy3-conjugated donkey anti-rabbit secondary antibody or Alexa Fluor 488-conjugated AffiniPure donkey anti-rabbit secondary antibody. **Panel A**. GLUT7 appears in red, with high prevalence on apical side. Cell membrane marker WGA appears in green. **Panel B**. In the absence of a cell membrane marker, GLUT7 appears in green, predominantly on the apical side. Scale bars (10 µm) are shown in the lower left corner of the first DAPI image in each panel and applies to all images. Images from left to right represent sections through the cell from the apical to basal side of the Caco-2/TC7 cell. Images are representative of 3 biological replicates.

Figure 2. Effect of sugars on GLUT7 mRNA and protein expression in differentiated Caco-2/TC7 intestinal cells. For analysis of mRNA, GLUT7 was multiplexed with TBP, and normalized to the glucose control. **Panel A**. Effect of sugars in apical compartment on GLUT7 mRNA expression. **Panel B**. Effect of sugars on apical and basolateral sides on GLUT7 mRNA expression. **Panel C.** GLUT7 and Na^+K^+ATPase protein detection in Caco-2/TC7 lysate, loaded at 0.5 mg protein/ml. **Panel D**: Standard curve showing peak area of GLUT7 and Na^+K^+ATPase against loaded protein concentration. GLUT7 and Na^+K^+ATPase antibody dilutions were 1:10 and 1:100 respectively. Detected protein size for GLUT7 and Na^+K^+ATPase was 49 kDa and 101 kDa respectively. **Panel E**. Effect of sugars on GLUT7 protein, multiplexed with Na^+/K^+ ATPase. **Panel F**. Effect of sugars on GLUT7 surface protein expression as assessed by biotinylation. Data points represent the mean of 3 biological replicates and three **(A, B)** or two **(E, F)** technical replicates, analysed in triplicate, ± SEM, with all data normalised to the glucose treatment. * $p \leq 0.05$, *** $p \leq 0.001$.

Figure 3. Exogenous expression of GLUT2, GLUT5 and GLUT7 proteins in membranes of Xenopus laevis oocytes. Membranes extracted from injected oocytes after 24 h (GLUT5), 48 h (GLUT2), or 120 h (GLUT7), as well as water-injected control membranes, were analysed using automated capillary Western blotting (WES). Data are shown as electropherograms for GLUT2 **(A)**, GLUT5 **(B)** and GLUT7 **(C)** and as gel image view for GLUT2 **(D)**, GLUT5 **(E)** and GLUT7 **(F)**. Detected protein sizes for GLUT2 and GLUT5 were 53 kDa and 60 kDa, respectively; GLUT7 was 48 kDa, following PNGase treatment. Mock PNGase represents un-digested samples.

Figure 4 Functionality of GLUT transporters expressed in Xenopus laevis oocytes. One day post GLUT5 mRNA microinjection, oocytes were incubated in 6 mM D-[^{14}C(U)]-fructose with and without 6 mM L-sorbose-Bn-OZO for 15 min **(A)**. Two days post GLUT2 mRNA microinjection **(B)** or five days post GLUT7 mRNA microinjection **(C),** oocytes were incubated in 0.1 mM D-[^{14}C(U)]-glucose with and without either 100 µM phloretin or 100 µM cytochalasin B (cytoB) for 5 min. Sugar uptake was determined by scintillation counting for oocytes expressing protein (black bars) and water injected controls (open bars). Net uptake (grey bars) was determined by normalizing the uptake observed by GLUT2, GLUT5 or GLUT7 injected oocytes against water-injected oocytes. The mean ± SEM of 6 replicates (18 oocytes) is shown per individual condition. ** $p \leq 0.01$ and **** $p \leq 0.0001$.

Figure 5 Effects of flavonoids on glucose and fructose uptake by Xenopus laevis oocytes expressing GLUT2. Two days post mRNA microinjection, oocytes were incubated in either 0.1 mM D-[^{14}C(U)]-glucose (left axis, ●) or 0.1 mM D-[^{14}C(U)]-fructose (right axis, ○) with EGCG **(A)**, apigenin **(B)** or quercetin **(C)** for 5 min, and sugar uptake determined by scintillation counting. Each data point represents the mean ± SEM of six mRNA-injected

replicates (18 oocytes) normalized to respective water-injected controls, incubated in the same conditions. * $p \leq 0.05$, ** $p \leq 0.01$, *** $p \leq 0.001$ and **** $p \leq 0.0001$.

Figure 6 Effects of flavonoids on fructose uptake by Xenopus laevis oocytes expressing GLUT5. One day post mRNA microinjection, oocytes were incubated in 0.1 mM D-[^{14}C(U)]-fructose with EGCG **(A)**, apigenin **(B)** and quercetin **(C)** for 5 min. Sugar uptake was determined by scintillation counting. Each data point represents the mean ± SEM of six mRNA-injected replicates (18 oocytes) normalized to respective water-injected controls, incubated in the same conditions. ** $p \leq 0.01$.

Figure 7 Effects of flavonoids on glucose and fructose uptake by Xenopus laevis oocytes expressing GLUT7. Five days post mRNA microinjection, oocytes were incubated in either 0.1 mM D-[^{14}C(U)]-glucose, or 0.1 mM D-[^{14}C(U)]-fructose, in the presence of EGCG **(A)** or quercetin **(C)** for 30 min. Oocytes were also incubated in 0.1 mM D-[^{14}C(U)]-glucose (left axis, ●) or 0.1 mM D-[^{14}C(U)]-fructose (right axis, ○) with apigenin **(B)** for 30 min. Internalized sugar uptake was determined by scintillation counting. Each data point represents the mean ± SEM of three mRNA-injected replicates (30 oocytes) **(A, C)** or six mRNA-injected replicates (60 oocytes) **(B)** normalised to respective water-injected controls, incubated in the same conditions. * $p \leq 0.05$.

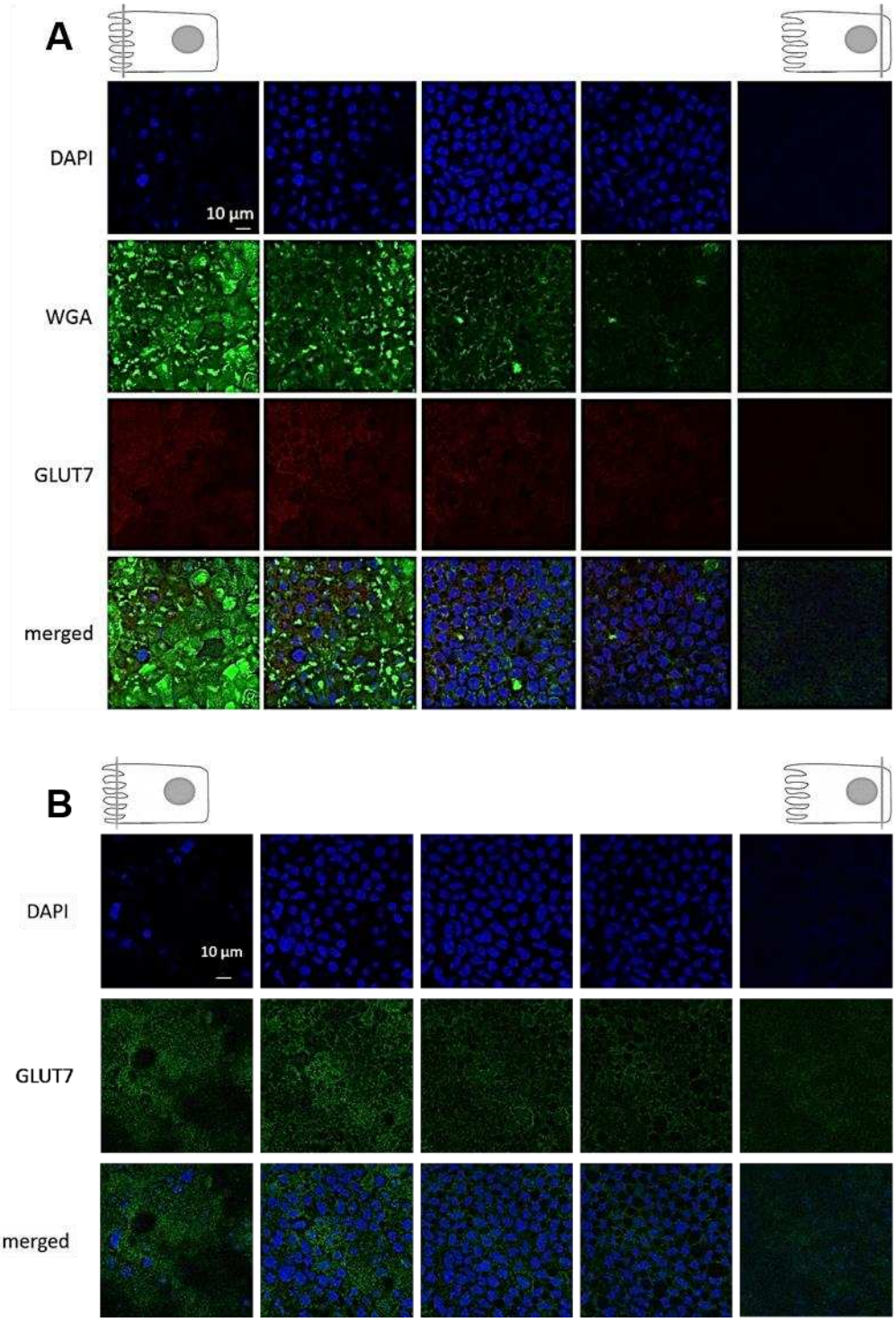

Figure 1

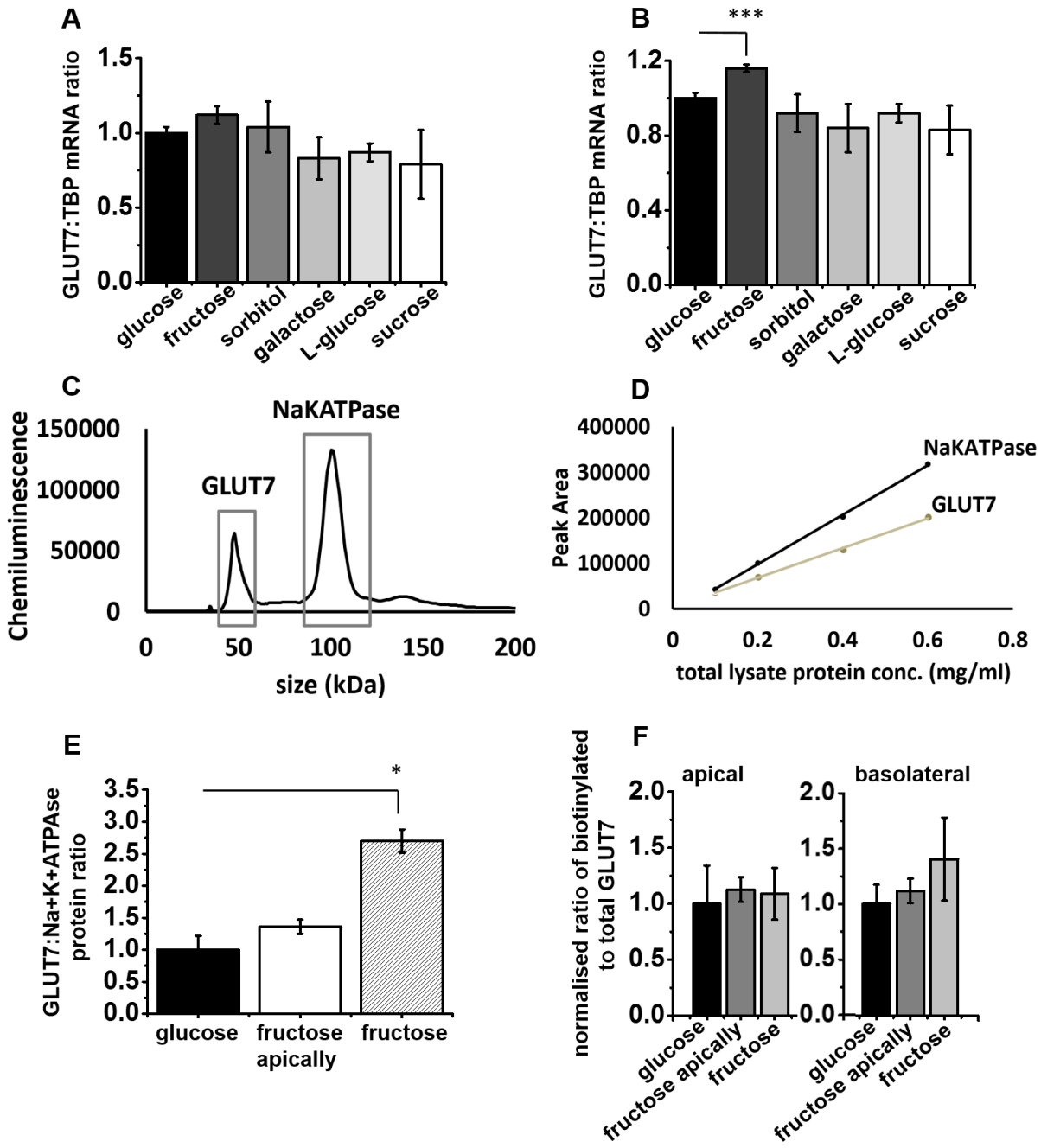
A
GLUT7:TBP mRNA ratio
1.5
1.0
0.5
0.0
glucose
fructose
sorbitol
galactose
L-glucose
sucrose
B
***
GLUT7:TBP mRNA ratio
1.2
0.8
0.4
0.0
glucose
fructose
sorbitol
galactose
L-glucose
sucrose
C
NaKATPase
GLUT7
Chemiluminescence
150000
100000
50000
0
0
50
100
150
200
size (kDa)
D
Peak Area
400000
300000
200000
100000
0
NaKATPase
GLUT7
0
0.2
0.4
0.6
0.8
total lysate protein conc. (mg/ml)
E
*
GLUT7:Na+K+ATPase protein ratio
3.5
3.0
2.5
2.0
1.5
1.0
0.5
0.0
glucose
fructose apically
fructose
F
apical
basolateral
normalised ratio of biotinylated to total GLUT7
2.0
1.5
1.0
0.5
0.0
glucose
fructose apically
fructose
glucose
fructose apically
fructose

Figure 2

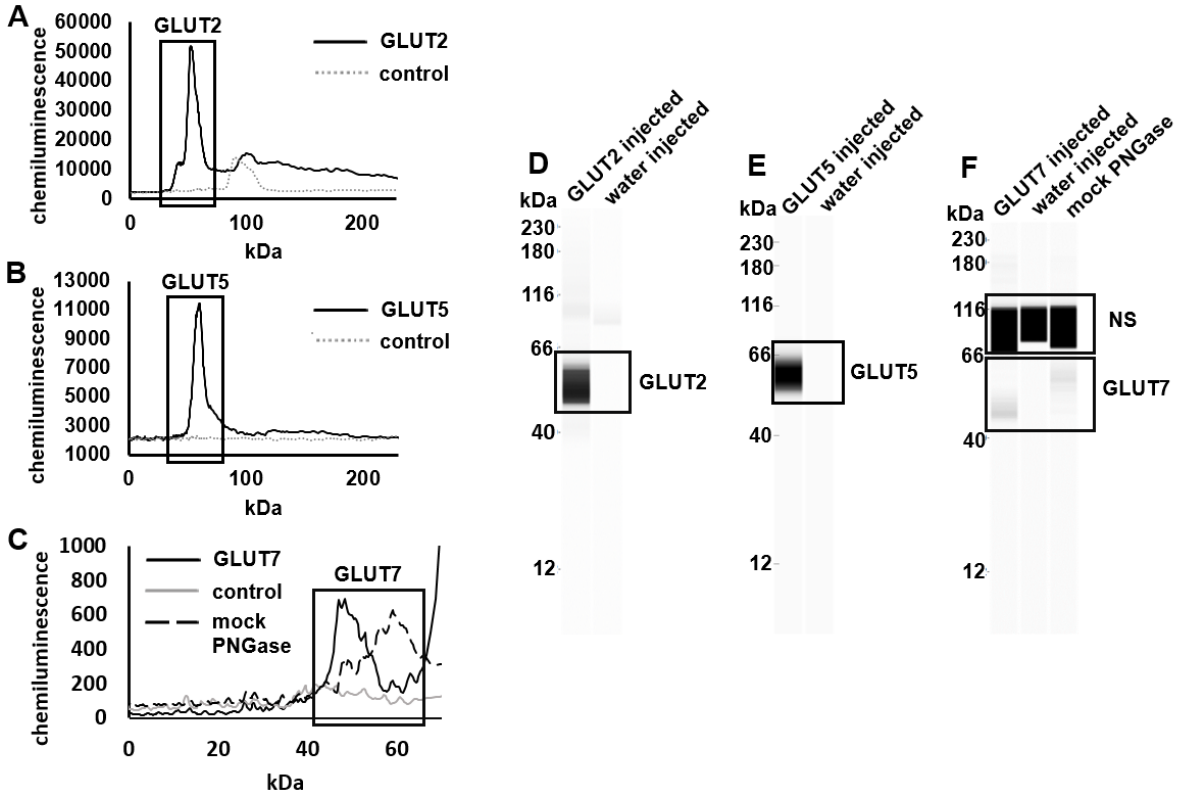
A
chemiluminescence
60000
50000
40000
30000
20000
10000
0
GLUT2
GLUT2
control
0
100
200
kDa
B
chemiluminescence
13000
11000
9000
7000
5000
3000
1000
GLUT5
GLUT5
control
0
100
200
kDa
C
chemiluminescence
1000
800
600
400
200
0
GLUT7
control
mock PNGase
GLUT7
0
20
40
60
kDa
D
GLUT2 injected
water injected
kDa
230
180
116
66
40
12
GLUT2
E
GLUT5 injected
water injected
kDa
230
180
116
66
40
12
GLUT5
F
GLUT7 injected
water injected
mock PNGase
kDa
230
180
116
66
40
12
NS
GLUT7

Figure 3

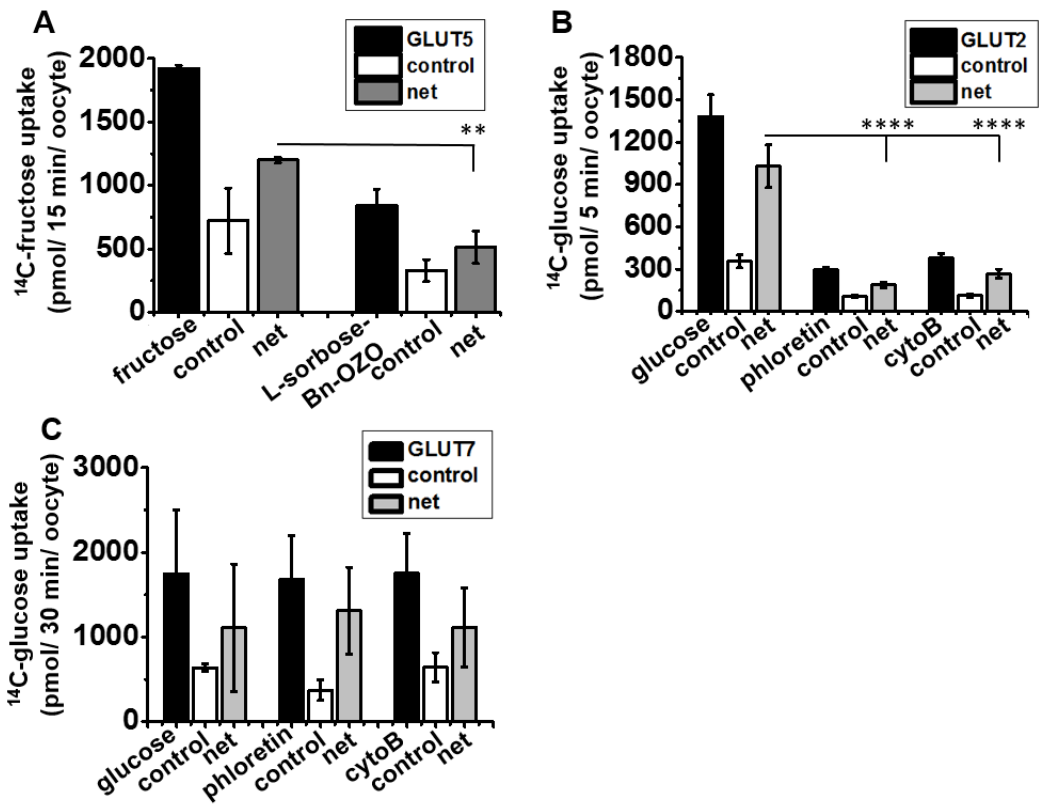
A
GLUT5
control
net
^{14}C-fructose uptake
(pmol/ 15 min/ oocyte)
2000
1500
1000
500
0
**
fructose
control
net
L-sorbose-
Bn-OZO
control
net
B
GLUT2
control
net
^{14}C-glucose uptake
(pmol/ 5 min/ oocyte)
1800
1500
1200
900
600
300
0
****
****
glucose
control
net
phloretin
control
net
cytoB
control
net
C
GLUT7
control
net
^{14}C-glucose uptake
(pmol/ 30 min/ oocyte)
3000
2000
1000
0
glucose
control
net
phloretin
control
net
cytoB
control
net

Figure 4

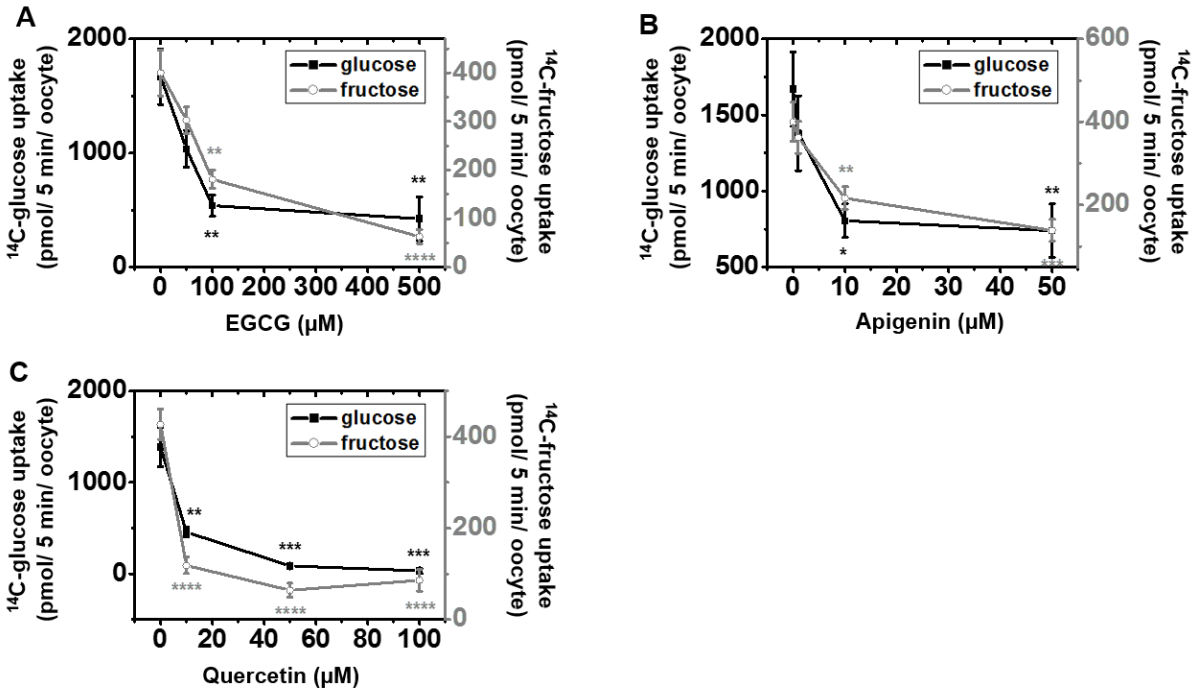
A
2000
1000
0
400
300
200
100
0
glucose
fructose
**
**
**
****
0 100 200 300 400 500
EGCG (μM)
14C-glucose uptake (pmol/ 5 min/ oocyte)
14C-fructose uptake (pmol/ 5 min/ oocyte)
B
2000
1500
1000
500
600
400
200
glucose
fructose
**
*
**
0 10 20 30 40 50
Apigenin (μM)
14C-glucose uptake (pmol/ 5 min/ oocyte)
14C-fructose uptake (pmol/ 5 min/ oocyte)
C
2000
1000
0
400
200
0
glucose
fructose
**
***
***
****
****
****
0 20 40 60 80 100
Quercetin (μM)
14C-glucose uptake (pmol/ 5 min/ oocyte)
14C-fructose uptake (pmol/ 5 min/ oocyte)

Figure 5

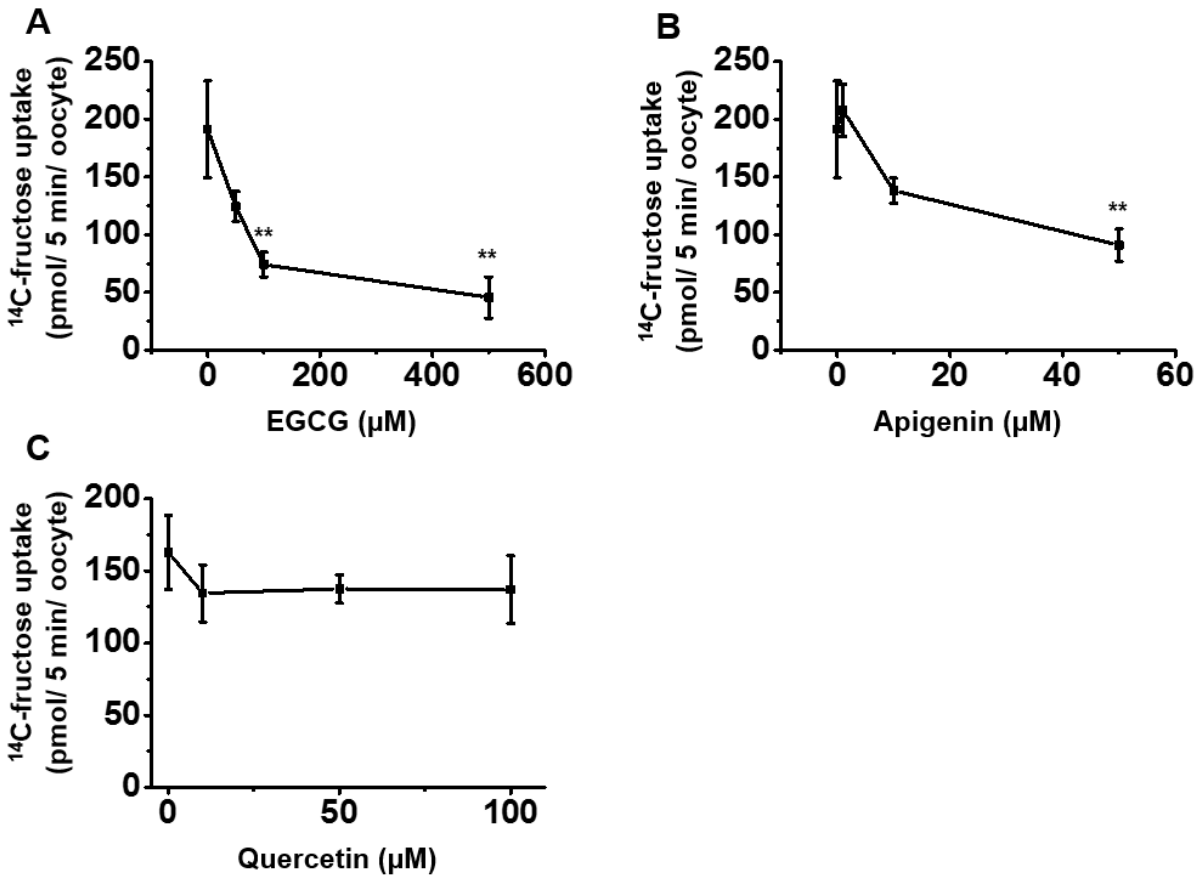
A
B
C
14C-fructose uptake (pmol/ 5 min/ oocyte)
EGCG (μM)
Apigenin (μM)
Quercetin (μM)
**
**
**
0
50
100
150
200
250
0
200
400
600
0
20
40
60
0
50
100

Figure 6

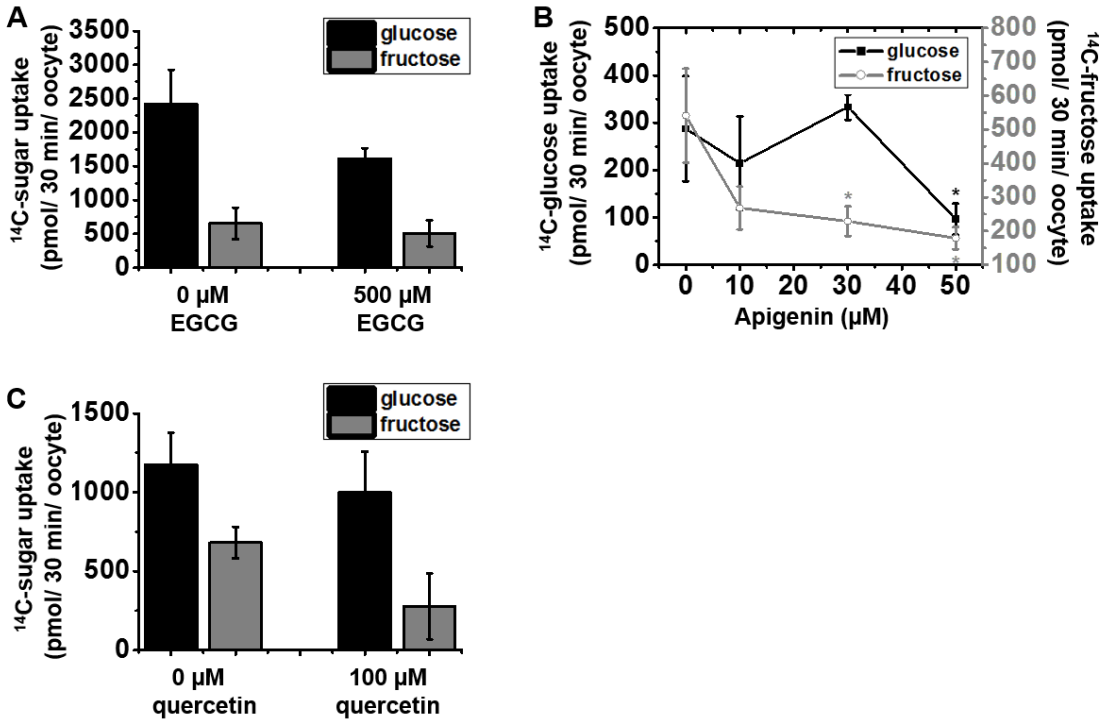
A
^{14}C-sugar uptake (pmol/ 30 min/ oocyte)
3500
3000
2500
2000
1500
1000
500
0
glucose
fructose
0 μM EGCG
500 μM EGCG
B
^{14}C-glucose uptake (pmol/ 30 min/ oocyte)
500
400
300
200
100
0
^{14}C-fructose uptake (pmol/ 30 min/ oocyte)
800
700
600
500
400
300
200
100
glucose
fructose
0
10
20
30
40
50
Apigenin (μM)
C
^{14}C-sugar uptake (pmol/ 30 min/ oocyte)
1500
1000
500
0
glucose
fructose
0 μM quercetin
100 μM quercetin

Figure 7

6. REFERENCES

[1] M.A. Hediger, M.J. Coady, T.S. Ikeda, E.M. Wright, Expression cloning and cDNA sequencing of the Na+/glucose co-transporter, Nature 330(6146) (1987) 379-81.

[2] K. Thorsen, T. Drengstig, P. Ruoff, Transepithelial glucose transport and Na+/K+ homeostasis in enterocytes: an integrative model, Am J Physiol Cell Physiol 307(4) (2014) C320-37.

[3] R.P. Ferraris, Dietary and developmental regulation of intestinal sugar transport, The Biochemical journal 360(Pt 2) (2001) 265-76.

[4] G.L. Kellett, E. Brot-Laroche, O.J. Mace, A. Leturque, Sugar absorption in the intestine: the role of GLUT2, Annual review of nutrition 28 (2008) 35-54.

[5] P.A. Helliwell, M.G. Rumsby, G.L. Kellett, Intestinal sugar absorption is regulated by phosphorylation and turnover of protein kinase C betaII mediated by phosphatidylinositol 3-kinase- and mammalian target of rapamycin-dependent pathways, The Journal of biological chemistry 278(31) (2003) 28644-50.

[6] E. Morgan, O.J. Mace, J. Affleck, G. Kellett, Apical GLUT2 and Cav1.3: regulation of rat intestinal glucose and calcium absorption, The Journal of physiology 580(2) (2007) 593-604.

[7] C.F. Burant, J. Takeda, E. Brot-Laroche, G.I. Bell, N.O. Davidson, Fructose transporter in human spermatozoa and small intestine is GLUT5, The Journal of biological chemistry 267(21) (1992) 14523-6.

[8] J. Girniene, A. Tatibouet, A. Sackus, J. Yang, G.D. Holman, P. Rollin, Inhibition of the D-fructose transporter protein GLUT5 by fused-ring glyco-1,3-oxazolidin-2-thiones and -oxazolidin-2-ones, Carbohydr Res 338(8) (2003) 711-9.

[9] S. Kane, M.J. Seatter, G.W. Gould, Functional studies of human GLUT5: effect of pH on substrate selection and an analysis of substrate interactions, Biochemical and biophysical research communications 238(2) (1997) 503-5.

[10] A.R. Manolescu, K. Witkowska, A. Kinnaird, T. Cessford, C. Cheeseman, Facilitated hexose transporters: new perspectives on form and function, Physiology (Bethesda, Md.) 22 (2007) 234-40.

[11] G.L. Kellett, E. Brot-Laroche, Apical GLUT2: a major pathway of intestinal sugar absorption, Diabetes 54(10) (2005) 3056-62.

[12] Q. Li, A. Manolescu, M. Ritzel, S. Yao, M. Slugoski, J.D. Young, X.Z. Chen, C.I. Cheeseman, Cloning and functional characterization of the human GLUT7 isoform SLC2A7 from the small intestine, Am J Physiol Gastrointest Liver Physiol 287(1) (2004) G236-42.

[13] A. Scheepers, S. Schmidt, A. Manolescu, C.I. Cheeseman, A. Bell, C. Zahn, H.G. Joost, A. Schurmann, Characterization of the human SLC2A11 (GLUT11) gene: alternative promoter usage, function, expression, and subcellular distribution of three isoforms, and lack of mouse orthologue, Molecular membrane biology 22(4) (2005) 339-51.

[14] L.A. Drozdowski, A.B. Thomson, Intestinal sugar transport, World journal of gastroenterology : WJG 12(11) (2006) 1657-70.

[15] C. Cheeseman, GLUT7: a new intestinal facilitated hexose transporter, Am J Physiol Endocrinol Metab 295(2) (2008) E238-41.

[16] A.J. Cura, A. Carruthers, Role of monosaccharide transport proteins in carbohydrate assimilation, distribution, metabolism, and homeostasis, Comprehensive Physiology 2(2) (2012) 863-914.

[17] K. Ebert, M. Ludwig, K.E. Geillinger, G.C. Schoberth, J. Essenwanger, J. Stolz, H. Daniel, H. Witt, Reassessment of GLUT7 and GLUT9 as Putative Fructose and Glucose Transporters, J Membr Biol 250(2) (2017) 171-182.

[18] K. Ebert, M. Ewers, I. Bisha, S. Sander, T. Rasputniac, H. Daniel, I. Antes, H. Witt, Identification of essential amino acids for glucose transporter 5 (GLUT5)- mediated fructose transport, J Biol Chem (2017).

[19] A. Manolescu, A.M. Salas-Burgos, J. Fischbarg, C.I. Cheeseman, Identification of a hydrophobic residue as a key determinant of fructose transport by the facilitative hexose transporter SLC2A7 (GLUT7), J Biol Chem 280(52) (2005) 42978-83.

[20] H. Doege, A. Bocianski, A. Scheepers, H. Axer, J. Eckel, H.G. Joost, A. Schurmann, Characterization of human glucose transporter (GLUT) 11 (encoded by SLC2A11), a novel sugar-transport facilitator specifically expressed in heart and skeletal muscle, The Biochemical journal 359(Pt 2) (2001) 443-9.

[21] T. Goto, M. Horita, H. Nagai, A. Nagatomo, N. Nishida, Y. Matsuura, S. Nagaoka, Tiliroside, a glycosidic flavonoid, inhibits carbohydrate digestion and glucose absorption in the gastrointestinal tract, Molecular nutrition & food research 56(3) (2012) 435-45.

[22] J.A. Villa-Rodriguez, E. Aydin, J.S. Gauer, A. Pyner, G. Williamson, A. Kerimi, Green and Chamomile Teas, but not Acarbose, Attenuate Glucose and Fructose Transport via Inhibition of GLUT2 and GLUT5, Molecular nutrition & food research (2017).

[23] O. Kwon, P. Eck, S. Chen, C.P. Corpe, J.H. Lee, M. Kruhlak, M. Levine, Inhibition of the intestinal glucose transporter GLUT2 by flavonoids, FASEB journal : official publication of the Federation of American Societies for Experimental Biology 21(2) (2007) 366-77.

[24] K. Johnston, P. Sharp, M. Clifford, L. Morgan, Dietary polyphenols decrease glucose uptake by human intestinal Caco-2 cells, FEBS Lett 579(7) (2005) 1653-1657.

[25] J. Song, O. Kwon, S. Chen, R. Daruwala, P. Eck, J.B. Park, M. Levine, Flavonoid inhibition of sodium-dependent vitamin C transporter 1 (SVCT1) and glucose transporter isoform 2 (GLUT2), intestinal transporters for vitamin C and Glucose, The Journal of biological chemistry 277(18) (2002) 15252-60.

[26] K. Slavic, E.T. Derbyshire, R.J. Naftalin, S. Krishna, H.M. Staines, Comparison of effects of green tea catechins on apicomplexan hexose transporters and mammalian orthologues, Mol Biochem Parasitol 168(1) (2009) 113-116.

[27] G.P. McDermott, D. Do, C.M. Litterst, D. Maar, C.M. Hindson, E.R. Steenblock, T.C. Legler, Y. Jouvenot, S.H. Marrs, A. Bemis, P. Shah, J. Wong, S. Wang, D. Sally, L. Javier, T. Dinio, C. Han, T.P. Brackbill, S.P. Hodges, Y. Ling, N. Klitgord, G.J. Carman, J.R. Berman, R.T. Koehler, A.L. Hiddessen, P. Walse, L. Bousse, S. Tzonev, E. Hefner, B.J. Hindson, T.H. Cauly, 3rd, K. Hamby, V.P. Patel, J.F. Regan, P.W. Wyatt, G.A. Karlin-Neumann, D.P. Stumbo, A.J. Lowe, Multiplexed target detection using DNA-binding dye chemistry in droplet digital PCR, Analytical chemistry 85(23) (2013) 11619-27.

[28] K. Ziegler, A. Kerimi, L. Poquet, G. Williamson, Butyric acid increases transepithelial transport of ferulic acid through upregulation of the monocarboxylate transporters SLC16A1 (MCT1) and SLC16A3 (MCT4), Arch Biochem Biophys 599 (2016) 3-12.

[29] H. Lodish, A. Berk, C. Kaiser, M. Kreiger, M. Scott, A. Bretscher, H. Ploegh, P. Matsudaira, Molecular Cell Biology, 6th ed., Freemand and Company, New York, NY, 2008.

[30] M. Mueckler, B. Thorens, The SLC2 (GLUT) family of membrane transporters, Mol Aspects Med 34(2-3) (2013) 121-38.

[31] B. Thorens, M. Mueckler, Glucose transporters in the 21st Century, Am J Physiol Endocrinol Metab 298(2) (2010) E141-5.

[32] R. Augustin, The protein family of glucose transport facilitators: It's not only about glucose after all, IUBMB Life 62(5) (2010) 315-33.

[33] A.R. Manolescu, R. Augustin, K. Moley, C. Cheeseman, A highly conserved hydrophobic motif in the exofacial vestibule of fructose transporting SLC2A proteins acts as a critical determinant of their substrate selectivity, Molecular membrane biology 24(5-6) (2007) 455-63.

[34] D. O'Connell, K. Mruk, J.M. Rocheleau, W.R. Kobertz, Xenopus laevis oocytes infected with multi-drug-resistant bacteria: implications for electrical recordings, The Journal of general physiology 138(2) (2011) 271-7.

[35] B. Legeza, Z. Balazs, A. Odermatt, Fructose promotes the differentiation of 3T3-L1 adipocytes and accelerates lipid metabolism, FEBS letters 588(3) (2014) 490-6.

[36] M. Cohen, D. Kitsberg, S. Tsytkin, M. Shulman, B. Aroeti, Y. Nahmias, Live imaging of GLUT2 glucose-dependent trafficking and its inhibition in polarized epithelial cysts, Open biology 4(7) (2014).

[37] M. Xu, J. Hu, W. Zhao, X. Gao, C. Jiang, K. Liu, B. Liu, F. Huang, Quercetin differently regulates insulin-mediated glucose transporter 4 translocation under basal and inflammatory conditions in adipocytes, Molecular nutrition & food research 58(5) (2014) 931-41.

[38] P. Strobel, C. Allard, T. Perez-Acle, R. Calderon, R. Aldunate, F. Leighton, Myricetin, quercetin and catechin-gallate inhibit glucose uptake in isolated rat adipocytes, The Biochemical journal 386(Pt 3) (2005) 471-8.